Preprints of the 19th World Congress
The International Federation of Automatic Control
Cape Town, South Africa. August 24-29, 2014

A Cross-Coupled Non-lifted Norm Optimal Iterative Learning Control Approach with Application to a Multi-axis Robotic Testbed

Heqing Sun*. Andrew G. Alleyne**

* Beijing Jiaotong University, Beijing, China (e-mail: sunheqingbjtu@gmail.com)
** University of Illinois at Urbana-Champaign, Urbana-Champaign, IL, USA
(Tel: 217 244 9993; e-mail: alleyne@illinois.edu)

Abstract: This paper combines previously developed non-lifted norm optimal iterative learning control (NNOILC)with a cross coupled formulation resulting in a cross-coupled non-lifted norm optimal iterative learning control (cross-coupled NNOILC). The objective is to improve the contour tracking performance in precision motion control of multi-axis systems while retaining the computational efficiency properties of the NNOILC. The NNOILC is able to provide many of the same design advantages of norm optimal ILC (NOILC) without the restrictions on trial size. Convergence and robustness properties are provided and shown to be similar to previous efforts in NNOILC. To demonstrate the proposed approach, experiments on a multi-axis robotic testbed are given.

1. INTRODUCTION

In all modern manufacturing systems, precision motion control is required to achieve high performance. In most multi-axis systems, individual controllers are designed for each motion axis. This may achieve highly accurate individual axis tracking but, if the axis bandwidths are mismatched, it may result in unsatisfactory path following or contour tracking. To improve the control performance of contour tracking, a cross-coupled control (CCC) (Koren, 1980) formulation was developed (Tang & Landers, in press).

For many manufacturing systems, the same task is executed multiple times. Their repetitive feature allows the controller to learn from previous iteration to achieve better performance. Therefore, iterative learning control (ILC) (Arimoto, Kawamura & Miyazak, 1984) is a promising control method for these systems. To improve the performance of contour tracking, ILC was previously combined with CCC and applied to multi-axis systems resulting in an approach termed cross-coupled ILC (CCILC) (Barton & Alleyne, 2008; Barton et al., 2009). Subsequently, to get better transient behavior in the iteration domain, optimization-based CCILC approaches were further studied; in particular, a cross-coupled NOILC (Barton et al., 2008; Barton et al., 2011). These cross-coupled NOILC approaches (Barton et al., 2008; Barton et al., 2011) were formed on the basis of lifted system techniques (Phan & Longman, 1988; Moore, 1993). Similar to other lifted optimal ILC approaches (Amann, Owens & Rogers, 1996; Barton & Alleyne, 2011; Lee, Lee & Kim, 2000), supervectors and large lifted matrices are needed in the synthesis and implementation. These large lifted matrices in cross-coupled NOILC make it computationally costly, or even infeasible, in terms of compute time, and thus inhibit their applications (Rice & Verhaegen, 2010). To remove the computational complexity issues of standard lifted optimal ILC approaches, a non-lifted NOILC (NNOILC) approach (Sun & Alleyne, in press) was developed.

The work in this paper builds on the previous work (Sun & Alleyne, in press) to extend the NNOILC to deal specifically with the cross-coupled control problems of the multi-axis systems. By considering contour errors in the process of controller design, the proposed cross-coupled NNOILC approach is designed to minimize the combination of individual axis errors and contour error. Note that the improvement of contour error may result at the cost of individual axis tracking performance, which will be illustrated in the section of experiments.

The rest of this paper is outlined as follows. Section 2 presents the class of multi-axis systems considered in this paper and provides the definition of contour error with respect to individual axis errors. The cross-coupled NNOILC approach is developed in Section 3, along with its properties including: convergence, robustness, and computational complexity. Section 4 shows the experimental results of the cross-coupled NNOILC approach applied to a multi-axis robotic testbed. Section 5 concludes the paper.

2. CLASS OF SYSTEMS

The class of systems considered here is linear discrete-time multi-axis system, P , given as,

$$\boldsymbol{x}_j(k+1) = \mathbf{A}(k)\boldsymbol{x}_j(k) + \mathbf{B}(k)\boldsymbol{u}_j(k) , \tag{1}$$

where $k = 0,1,\cdots,N-1$ refers to the discrete-time index, the subscript $j = 1,2,\cdots$ is the iteration index, $\boldsymbol{u}_j(k) = \left[\boldsymbol{u}_{1,j}^T(k) \quad \cdots \quad \boldsymbol{u}_{M,j}^T(k)\right]^T \in \mathbb{R}^{q_i \cdot M}$ is the control input, $\boldsymbol{x}_j(k) = \left[\boldsymbol{x}_{1,j}^T(k) \quad \cdots \quad \boldsymbol{x}_{M,j}^T(k)\right]^T \in \mathbb{R}^{q_x \cdot M}$ is the system state, $\boldsymbol{u}_{i,j}(k), \boldsymbol{x}_{i,j}(k)$ are the input and state of the i-th axis, $i = 1,2,\cdots,M$, and $\mathbf{A}(k)$ and $\mathbf{B}(k)$ are appropriately sized iteration-invariant real-valued matrices.

In practice, most system models inevitably contain some form of model uncertainty. To address these uncertainties in our later controller design, we assume that the true system

$P_t(\mathbf{A}_t(k), \mathbf{B}_t(k))$ corresponds to the nominal model $P(\mathbf{A}(k), \mathbf{B}(k))$ with uncertainties, given in the form,

$$\mathbf{A}_t(k) = \mathbf{A}(k)(1+\mathbf{\Delta}_A(k)) \ , \tag{2}$$

$$\mathbf{B}_t(k) = \mathbf{B}(k)(1+\mathbf{\Delta}_B(k)) \ . \tag{3}$$

With the above uncertainty definition, the actual model of the multi-axis system can be described as,

$$\boldsymbol{x}_j(k+1) = \mathbf{A}_t(k)\boldsymbol{x}_j(k) + \mathbf{B}_t(k)\boldsymbol{u}_j(k) \ . \tag{4}$$

In Section 3, the cross-coupled NNOILC approach will be studied for both the nominal system in (1), as well as the true system given by (4).

2.1 Assumptions

For the purpose of analyzing the algorithm's properties, three reasonable assumptions are made here.

Assumption 1. The re-initialization condition is satisfied throughout the repeated iterations, i.e.,

$$\boldsymbol{x}_j(0) = \boldsymbol{x}_d(0), \ \forall \ j = 1, 2, \cdots \ , \tag{5}$$

where $\boldsymbol{x}_j(0)$ is the initial value of the system state at *j*-th iteration, and $\boldsymbol{x}_d(0)$ is the desired initial value of the system state.

Assumption 2. There exists an appropriate control input $\boldsymbol{u}_j(k)$, which drives the system state to track $\boldsymbol{x}_d(k+1)$ over the finite interval $k \in [0, N-1]$, i.e.,

$$\boldsymbol{x}_d(k+1) = \mathbf{A}(k)\boldsymbol{x}_d(k) + \mathbf{B}(k)\boldsymbol{u}_d(k) \ . \tag{6}$$

Assumption 3. Both the true and nominal plants, $P_t(\mathbf{A}_t(k), \mathbf{B}_t(k))$, $P(\mathbf{A}(k), \mathbf{B}(k))$, are stable or can be readily stabilized via feedback.

2.2 Contour Error

To guarantee the completeness of this paper, the contour error is briefly defined here. The interested reader can refer to Tang & Landers (in press) for further details.

Contour error is a function of individual axis errors and time. For a general class of multi-axis systems, contour error can be defined as a linear approximation of the closest distance from the actual position to the instantaneous tangent line of the reference trajectory with respect to time. Specifically, for two-axis systems, contour error can be defined as,

$$\varepsilon(k) = \boldsymbol{c}_1(\theta, k) \cdot \boldsymbol{e}_1(k) + \boldsymbol{c}_2(\theta, k) \cdot \boldsymbol{e}_2(k) \ , \tag{7}$$

where $\varepsilon(k)$ is the contour error, $\boldsymbol{e}_i(k)$ ($i = 1, 2$) is the individual axis error, $\boldsymbol{c}_i(\theta, k)$ ($i = 1, 2$) is the coupling gain and is used to define the contour error with respect to the individual axis errors, and θ is the instantaneous angle of the reference trajectory with respect to the *1*st axis of the two-axis system. The coupling gains are generally time-varying gains that change with respect to the desired trajectory. Linearized coupling gains have the following format,

$$c_1(\theta, k) = -\sin\theta(k); \ \ c_2(\theta, k) = \cos\theta(k) \ . \tag{8}$$

Note that the use of trajectory-dependent coupling gains leads to a time-varying controller. Define $\boldsymbol{e}(k) = [e_1(k), e_2(k)]^T$, $\boldsymbol{c}(\theta, k) = [-\sin\theta(k), \cos\theta(k)]^T$, and contour error (7) can be rewritten into the following compact form,

$$\varepsilon(k) = \boldsymbol{c}^T(\theta, k) \cdot \boldsymbol{e}(k) \ . \tag{9}$$

3. CROSS-COUPLED NON-LIFTED NOILC

In this section, we consider the multi-axis system given in (1) to develop cross-coupled NNOILC approach and analyze its properties.

The basis of the proposed approach is to minimize the following cost function,

$$\begin{aligned} J_j(k) = {} & Q_{co}\varepsilon_j^2(k+1) + \boldsymbol{e}_j^T(k+1)\mathbf{Q}_{in}\boldsymbol{e}_j(k+1) \\ & + \Delta\boldsymbol{u}_j^T(k)\mathbf{R}\Delta\boldsymbol{u}_j(k) + \boldsymbol{u}_j^T(k)\mathbf{S}\boldsymbol{u}_j(k) \ , \end{aligned} \tag{10}$$

where $\boldsymbol{e}_j(k) = \boldsymbol{x}_d(k) - \boldsymbol{x}_j(k)$ denotes the state errors, i.e., individual axis errors, at sample index *k* of the system in the *j*-th iteration, $\varepsilon_j(k)$ represents the contour error at sample index *k* of the system in the *j*-th iteration, and $\Delta\boldsymbol{u}_j(k) = \boldsymbol{u}_j(k) - \boldsymbol{u}_{j-1}(k)$ is the "slew rate" of the control input along iteration axis. The individual axis gain $\mathbf{Q}_{in}$ and cross-coupled gain Q_{co} refer to the weighting gains applied to individual axis errors and contour error, respectively. Moreover, weighting matrices $\mathbf{Q}_{in}, \mathbf{R}, \mathbf{S}$ and weighting factor Q_{co} are chosen to satisfy the convergence or robust condition in the theorems in Section 3.

Note that unlike existing cross-coupled NOILC approaches (Barton et al., 2008; Barton et al., 2011), the cost function (10) only contains the information at an individual sample time within an iteration, rather than the entire trial's error and input. In addition, comparing with non-lifted NOILC (Sun & Alleyne, in press) for individual axis motion control, a penalty term on contour error $\varepsilon_j(k+1)$ is added, which will make the controller gain the extra performance benefits of contour tracking.

Substituting (9) into (10) results in,

$$\begin{aligned} J_j(k) = {} & \boldsymbol{e}^T(k+1)\mathbf{Q}(k)\boldsymbol{e}(k+1) + \Delta\boldsymbol{u}_j^T(k)\mathbf{R}\Delta\boldsymbol{u}_j(k) \\ & + \boldsymbol{u}_j^T(k)\mathbf{S}\boldsymbol{u}_j(k) \ , \end{aligned} \tag{11}$$

where $\mathbf{Q}(k) = \mathbf{Q}_{in} + Q_{co} \cdot \boldsymbol{c}(\theta, k+1)\boldsymbol{c}^T(\theta, k+1)$. Note that after introducing the penalty term on contour error, the weighting matrix $\mathbf{Q}(k)$ becomes a time-varying matrix.

Differencing the system model (1) along the iteration axis gives,

$$\boldsymbol{x}_j(k+1) = \boldsymbol{x}_{j-1}(k+1) + \mathbf{A}(k)\Delta\boldsymbol{x}_j(k) + \mathbf{B}(k)\Delta\boldsymbol{u}_j(k) \ , \tag{12}$$

where $\Delta\boldsymbol{x}_j(k) = \boldsymbol{x}_j(k) - \boldsymbol{x}_{j-1}(k)$. Substituting (12) into (11), and using the optimality condition $\frac{1}{2}\frac{\partial J_j(k)}{\partial \boldsymbol{u}_j(k)} = 0$, we can obtain the cross-coupled NNOILC update law as follows,

$$\boldsymbol{u}_j(k) = \boldsymbol{L}_u(k)\boldsymbol{u}_{j-1}(k) + \boldsymbol{L}_e(k)\boldsymbol{e}_{j-1}(k+1) - \boldsymbol{L}_x(k)\Delta\boldsymbol{x}_j(k) \ . \tag{13}$$

In (13),

$$\boldsymbol{L}_u(k) = \left(\boldsymbol{B}^T(k)\mathbf{Q}(k)\boldsymbol{B}(k) + \mathbf{R} + \mathbf{S}\right)^{-1} \times \left(\boldsymbol{B}^T(k)\mathbf{Q}(k)\boldsymbol{B}(k) + \mathbf{R}\right), \tag{14}$$

$$\boldsymbol{L}_e(k) = \left(\boldsymbol{B}^T(k)\mathbf{Q}(k)\boldsymbol{B}(k) + \mathbf{R} + \mathbf{S}\right)^{-1} \boldsymbol{B}^T(k)\mathbf{Q}(k), \tag{15}$$

$$\boldsymbol{L}_x(k) = \boldsymbol{L}_e(k)\mathbf{A}(k). \tag{16}$$

From (13), we find that the dimensions of the matrices in the cross-coupled NNOILC update law depend only on the plant model and have no relation to the trial length.

Remark 1. Since the weighting matrix $\mathbf{Q}(k)$ contains penalties on both individual axis errors and contour error, the proposed cross-coupled NNOILC update law (13) would make a tradeoff between individual axis tracking and contour tracking by selecting different individual axis gain $\mathbf{Q}_{in}$ and cross-coupled gain Q_{co}.

Rewriting (13) yields,

$$\boldsymbol{u}_j(k) = \boldsymbol{L}_u(k)\boldsymbol{u}_{j-1}(k) + \boldsymbol{L}_e(k)\boldsymbol{e}_{j-1}(k+1) + \boldsymbol{L}_x(k)\left(\boldsymbol{e}_j(k) - \boldsymbol{e}_{j-1}(k)\right). \tag{17}$$

Equation (17) shows that the structure of the proposed cross-coupled NNOILC update law is conceptually similar to a PD-type ILC, but here the D-term is the difference along the iteration axis rather than the time axis.

Remark 2. The proposed cross-coupled NNOILC update law (17) includes information fed back from both the current iteration and previous iteration. This would indicate that it has similarities to some of the current iteration ILC algorithms. Therefore, according to the discussion in Bristow, Tharayil, & Alleyne (2006) and the references therein, the proposed cross-coupled NNOILC approach will benefit from the performance improvement afforded by the learned feedforward as well as robustness benefits afforded by the feedback element.

The rest of this section focuses on the relevant properties of the proposed cross-coupled NNOILC approach with respect to nominal convergence, robust convergence, and computational complexity.

The following two theorems explore the asymptotic and monotonic convergence for the nominal plant model (1).

Theorem 1. If the system (1) ($k = 0,1,\cdots,N-1$) is controlled by the cross-coupled NNOILC update law (13), the asymptotic convergence of the individual axis errors and contour error of the controlled system along the iteration axis is guaranteed by,

$$\lambda\left(\left(\mathbf{B}^T(k)\mathbf{Q}(k)\mathbf{B}(k) + \mathbf{R} + \mathbf{S}\right)^{-1}\mathbf{R}\right) < 1, \quad \forall\ k = 0,1,\cdots,N-1. \tag{18}$$

Proof. The proof of the asymptotic convergence of the individual axis errors is similar to the Theorem 1 in Sun & Alleyne (in press). Because the individual axis errors are asymptotic convergent along iteration axis, according to the relationship between the contour error and the individual axis error (7), the contour error is also asymptotically convergent along iteration axis.

ILC systems that are asymptotically convergent may still experience large transients in the iteration domain prior to convergence (Phan, Longman, & Moore, 2000). This may not be acceptable for several physical systems, such as motion control manufacturing platforms. Therefore, monotonic convergence is desirable, although requiring stricter conditions for learning gains.

Theorem 2. For the system (1), the presented cross-coupled NNOILC update law (13) can guarantee the controlled system to be monotonically convergent along the iteration axis with any symmetric positive definite weighting matrices $\mathbf{Q}(k), \mathbf{R}$ and a positive define $\mathbf{S}$ that ensures the following inequality:

$$\left\| \left(\mathbf{B}_{lift}^T \mathbf{Q}_{lift} \mathbf{P}_{lift} + \mathbf{R}_{lift} + \mathbf{S}_{lift}\right)^{-1} \mathbf{R}_{lift} \right\| < 1. \tag{19}$$

We define lifted system matrices,
$\mathbf{B}_{lift} = \begin{bmatrix} \mathbf{B}(0) & & \mathbf{0} \\ & \ddots & \\ \mathbf{0} & & \mathbf{B}(N-1) \end{bmatrix}$, $\mathbf{Q}_{lift} = \begin{bmatrix} \mathbf{Q}(0) & & \mathbf{0} \\ & \ddots & \\ \mathbf{0} & & \mathbf{Q}(N-1) \end{bmatrix}$,
$\mathbf{R}_{lift} = \begin{bmatrix} \mathbf{R} & & \mathbf{0} \\ & \ddots & \\ \mathbf{0} & & \mathbf{R} \end{bmatrix}$, $\mathbf{S}_{lift} = \begin{bmatrix} \mathbf{S} & & \mathbf{0} \\ & \ddots & \\ \mathbf{0} & & \mathbf{S} \end{bmatrix}$, $\mathbf{P}_{lift} = \begin{bmatrix} H_{0,0} & & 0 \\ \vdots & \ddots & \\ H_{N-1,0} & \cdots & H_{N-1,N-1} \end{bmatrix}$,

where $\mathbf{P}_{lift}$ is the convolution matrix of the system,

$$\mathbf{H}_{h,l} = \begin{cases} \mathbf{B}(h-1), & h = l, \\ \mathbf{A}(h-1)\cdots\mathbf{A}(l+1)\mathbf{B}(l), & h > l. \end{cases} \tag{20}$$

Proof. Similar to the Theorem 2 in Sun & Alleyne (in press).

Remark 3. If $\mathbf{R} = r\mathbf{I}$ ($r > 0$), the monotonic convergence condition can be further derived as,

$$\mathbf{B}_{lift}^T \mathbf{Q}_{lift} \mathbf{P}_{lift} + \mathbf{P}_{lift}^T \mathbf{Q}_{lift} \mathbf{B}_{lift} + 2\mathbf{S}_{lift} > 0. \tag{21}$$

From (21), a sufficiently large $\mathbf{S}$ can guarantee monotonic convergence.

The following two theorems study the robustness of the proposed cross-coupled NNOILC approach when considering the true system (4) with the uncertainties $\mathbf{\Delta}_A(k), \mathbf{\Delta}_B(k)$.

Theorem 3. Consider the true system (4) ($k = 0,1,\cdots,N-1$), with multiplicative uncertainties $\mathbf{\Delta}_A(k), \mathbf{\Delta}_B(k)$. If this system is controlled by the cross-coupled NNOILC update law (13), robust asymptotic convergence of the individual axis errors and contour error of the controlled system along the iteration domain is guaranteed by weighting matrices $\mathbf{Q}(k), \mathbf{R}, \mathbf{S}$ satisfying the following inequality,

$$\lambda\left(\left(\mathbf{B}^T(k)\mathbf{Q}(k)\mathbf{B}(k) + \mathbf{R} + \mathbf{S}\right)^{-1} \times \left(\mathbf{R} - \mathbf{B}^T(k)\mathbf{Q}(k)\mathbf{B}(k)\mathbf{\Delta}_B(k)\right)\right) < 1, \quad \forall\ k = 0,1,\cdots,N-1. \tag{22}$$

Proof. Similar to Theorem 1.

Remark 4. If $\mathbf{R} = r\mathbf{I}$ ($r > 0$), the robust asymptotic convergence condition (22) can be further simplified as,

$$\left\| \left(\mathbf{B}^T(k)\mathbf{Q}(k)\mathbf{B}(k) + \mathbf{S}\right)^{-1} \mathbf{B}^T(k)\mathbf{Q}(k)\mathbf{B}(k)\mathbf{\Delta}_B(k) \right\|_{i2} < 1. \tag{23}$$

The proof of (23) can reference Lemma 2 in Barton & Alleyne (2011). In addition, one can derive from (23) that a sufficiently large $\mathbf{S}$ can overcome model uncertainties, and achieve robustness.

Remark 5. For ILC systems, performance is defined in terms of the final steady state error to which the system converges. Similar to the analysis in Barton & Alleyne (2011), we can conclude that the minimum steady state error requires $\|\mathbf{S}\|_{i2} = 0$.

Combining Remark 4 and Remark 5, the weighting matrix $\mathbf{S}$ should provide a balance between the robustness and the performance of the system.

The robust convergence condition (22) is independent of uncertainty $\mathbf{\Delta}_A(k)$. However, this independence with respect to the system dynamics may result in poor transients for the cross-coupled NNOILC. Therefore, monotonic convergence is analyzed below.

Theorem 4. Consider the true system (4), controlled by the cross-coupled NNOILC update law (13). Robust monotonic convergence of the controlled system is guaranteed along the iteration domain by any weighting matrices $\mathbf{Q}(k), \mathbf{R}, \mathbf{S}$ satisfying the following inequality,

$$\begin{aligned}&\left\|\left(\mathbf{B}_{lift}^T\mathbf{Q}_{lift}\left(\mathbf{B}_{lift}+\mathbf{A}_{lift}\mathbf{\Psi}_{t,lift}\right)+\mathbf{R}_{lift}+\mathbf{S}_{lift}\right)^{-1}\right.\\ &\left.\quad\times\left(\mathbf{R}_{lift}-\mathbf{B}_{lift}^T\mathbf{Q}_{lift}\left(\mathbf{B}_{lift}\mathbf{\Delta}_{B,lift}+\mathbf{A}_{lift}\mathbf{\Delta}_{A,lift}\mathbf{\Psi}_{t,lift}\right)\right)\right\|<1\ .\end{aligned} \tag{24}$$

where $\mathbf{A}_{lift}=\begin{bmatrix}\mathbf{A}(0) & & \mathbf{0}\\ & \ddots & \\ \mathbf{0} & & \mathbf{A}(N-1)\end{bmatrix}$,

$$\mathbf{\Delta}_{B,lift}=\begin{bmatrix}\mathbf{\Delta}_B(0) & & \mathbf{0}\\ & \ddots & \\ \mathbf{0} & & \mathbf{\Delta}_B(N-1)\end{bmatrix},\ \mathbf{\Delta}_{A,lift}=\begin{bmatrix}\mathbf{\Delta}_A(0) & & \mathbf{0}\\ & \ddots & \\ \mathbf{0} & & \mathbf{\Delta}_A(N-1)\end{bmatrix},$$

$$\mathbf{\Psi}_{t,lift}=\begin{bmatrix}\mathbf{0} & \mathbf{0} & \cdots & & \cdots & \mathbf{0}\\ \mathbf{B}_t(0) & \ddots & \ddots & & & \vdots\\ \mathbf{A}_t(1)\mathbf{B}_t(0) & \ddots & \ddots & & \ddots & \vdots\\ \vdots & \ddots & \ddots & & \ddots & \mathbf{0}\\ \prod_{m=1}^{N-2}\mathbf{A}_t(m)\mathbf{B}_t(0) & \cdots & \mathbf{A}_t(N-2)\mathbf{B}_t(N-3) & & \mathbf{B}_t(N-2) & \mathbf{0}\end{bmatrix}.$$

Proof. Similar to Theorem 2.

Remark 6. The matrices used to check either the nominal monotonic convergence condition (19), (21) or robust monotonic convergence condition (24) are all in lifted form, which is not necessary for the asymptotic convergence cases. Therefore, the determination of monotonic convergence is still limited by the trial length as with existing cross-coupled NOILC approaches. There are two solutions. One is to choose $\mathbf{S}$ large enough, as mentioned in Remark 3 and Remark 4. The other one is to apply numerical techniques to minimize the complexity. One example is the implicitly restarted Arnoldi/Lanczos method (IRLM) which was utilized in Barton, Bristow, & Alleyne, (2010) to reduce the computational complexity to scale linearly with the trial length. While the convergence analysis is limited, it should be noted that the implementation of the cross-coupled NNOILC is still in a non-lifted form and so does not suffer from the complexity issues.

Finally, the computational complexity of the proposed approach will be discussed. A typical measure of computational complexity is the number of floating point operations, or flops. Similar to the analysis in subsection 3.3 in Sun & Alleyne (in press), the computational complexity of the presented cross-coupled NNOILC update law (13) and existing cross-coupled NOILC (Barton et al., 2008) in one iteration is *O(N)* and *O(N^3)*, respectively. Therefore, the proposed cross-coupled NNOILC approach is more efficient and applicable than existing cross-coupled NOILC for long trials.

4. EXPERIMENTS

In order to verify the effectiveness of the proposed cross-coupled NNOILC approach, a multi-axis robotic testbed is used. The h-bridge gantry style robotic system consists of stacked *x*, *y*, and *z* axes all mounted orthogonally to one another. This robotic system is used for manufacturing parts and devices with fine feature sizes via material addition or deposition as would occur in an additive manufacturing scheme. A picture is shown in Fig. 1 and more detailed description can be found in Bristow & Alleyne (2006) where the system was used for 3D additive manufacturing.

To illustrate the performance of the proposed approach clearly, our experiments here only focus on the movements of *x*- and *y*-axes.

For the controller design, dynamic models for the *x*- and *y*-axes were developed and feedback controllers were designed. Using a swept sine frequency response, 1-kHz sampled dynamic models of the *x*- and *y*-axes are,

$$G_x(z)=\frac{0.0172(z+0.759)(z^2-1.706z+0.9596)(z^2-0.0324z+0.8968)}{(z-0.9972)(z-1)(z^2-1.676z+0.9479)(z^2-0.3736+0.4904)}, \tag{25}$$

$$G_y(z)=\frac{0.0459(z+0.9963)(z^2-1.768z+0.9567)(z^2-0.2238z+0.7933)}{(z-0.9972)(z-1)(z^2-1.764z+0.9562)(z^2-0.1784+0.7898)}, \tag{26}$$

where z represents the z-transform of the discrete-time dynamics. The high performance feedback controllers that stabilize the *x*- and *y*-axes plant models (25) and (26) are,

$$C_x(z)=\frac{3.5(z-1.92)(z-0.8881)(z-0.8583)}{(z-1.001)(z-0.5185)(z-0.1691)}, \tag{27}$$

$$C_y(z)=\frac{1.5(z-1.377)(z-0.9147)(z-0.776)}{(z-1.001)(z-0.5185)(z-0.1691)}. \tag{28}$$

The reference signal applied to the system is a raster scanning trajectory ($N = 2000$), in which the motion consists of long periods of low frequency content followed by short periods of high frequency transitions with a sudden change in y axis direction. This type of trajectory is commonly used in atomic force microscopy (AFM), as well as other manufacturing systems which require sharp transitions between signals. Fig. 2. shows the overall raster trajectory as well as the individual *x*- and *y*-axes position reference plots. The circled points in Fig. 2 illustrate the most challenging points for contour tracking.

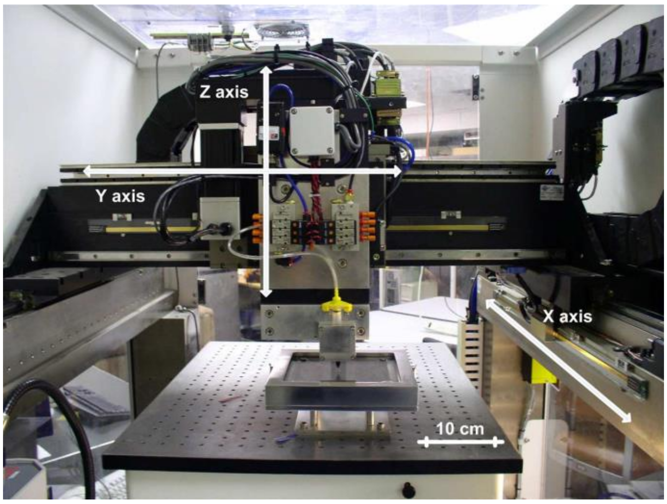

Fig. 1. Image of the multi-axis robotic testbed

To demonstrate the effectiveness of the proposed approach, the cross-coupled NNOILC approach is applied to the closed-loop system consisting of the x- and y-axis linear motors of robotic testbed and feedback controllers (27) and (28). Three different values of cross-coupled gain Q_{co} are applied here to compare their effects on the improvement of contour error: $Q_{co} = 0.2$, $Q_{co} = 0.5$ and $Q_{co} = 1$. The other controller parameters are chosen as $\mathbf{Q}_{in} = \begin{bmatrix} 0.5 & 0 \\ 0 & 0.5 \end{bmatrix}$, $\mathbf{R} = \begin{bmatrix} 0.0008 & 0 \\ 0 & 0.0002 \end{bmatrix}$, $\mathbf{S} = \begin{bmatrix} 0.0003 & 0 \\ 0 & 0.0002 \end{bmatrix}$, and $\boldsymbol{c}(\theta,k) = \left[-\sin\theta(k), \cos\theta(k)\right]^T$. All of these sets of weighting terms satisfy the convergence condition analyzed in Section 3.

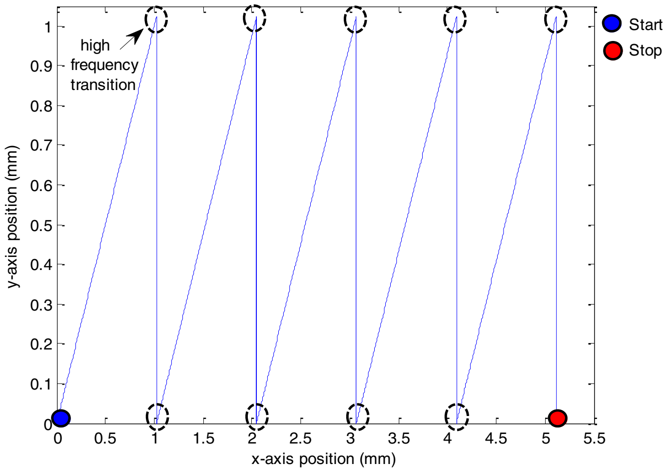

(a) Raster scan trajectory

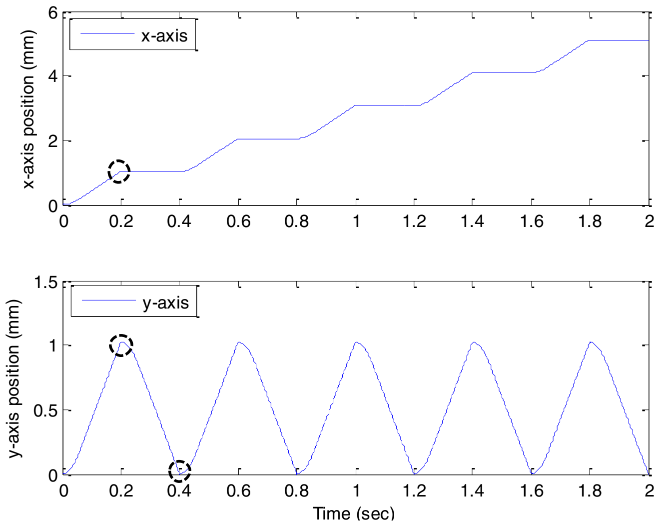

(b) Individual axis reference signals

Fig. 2. Reference trajectory

Fig. 3. gives the individual learning errors of the x- and y-axes with different cross-coupled learning gains. Fig. 4 shows the contour learning errors of the x- and y-axes with different cross-coupled gains. Individual axis learning error is defined as the root mean square (RMS) of the motor's position errors over the whole time interval for one iteration. Contour learning error is defined as the RMS of the contour errors over the whole time interval for one iteration.

As illustrated in Fig. 3, all of the individual axis learning errors with different cross-coupled gains converge in the iteration domain. As may be expected, the cross-coupled NNOILC provides a slightly worse performance when observing the behavior of the individual x- or y-axis. In fact, close examination indicates that the cross-coupled NNOILC approach achieves its coordination by improving the converged error of x-axis and deteriorating the converged error of y-axis. Fig. 4 illustrates that the cross-coupled NNOILC with larger cross-couple gain does a much better job when we evaluate the contour error of x- and y-axes. It is the deterioration of y-axis performance here that serves to provide greater benefit to the overall system coordination.

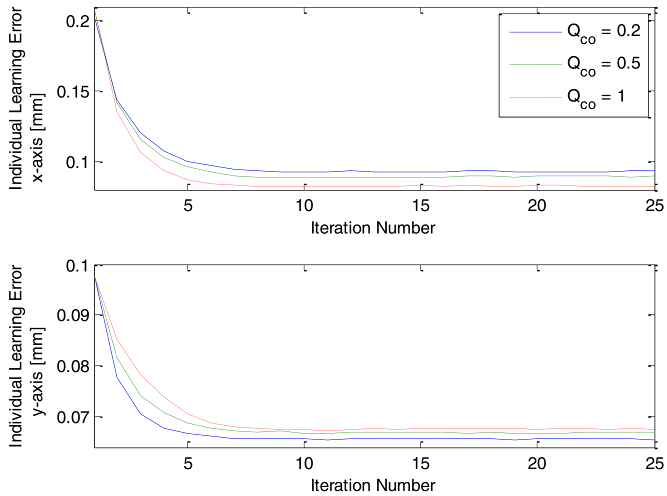

Fig. 3. Individual learning errors of cross-coupled NNOILC

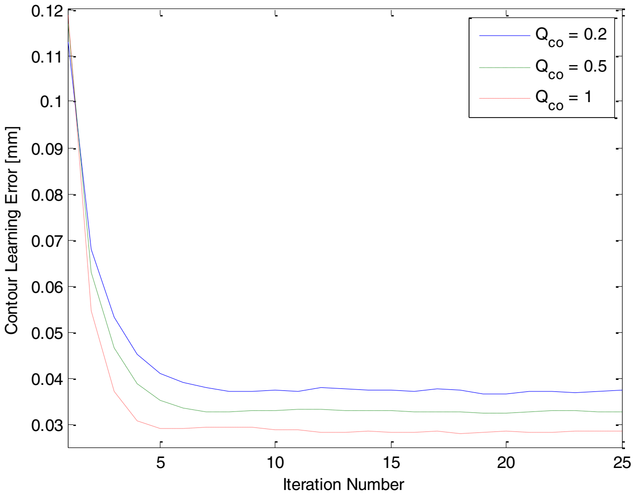

Fig. 4. Contour learning errors of cross-coupled NNOILC

The reason for this is evident when considering the design of the robot. The x-axis carries the y- and z- axes. Therefore, it has the highest inertia as evidenced in the open loop dynamics of (25) and (26). The linear motors driving the two axes are the same. Therefore, the y- axis has a higher closed loop bandwidth due to its lower inertia. The best way for the system to achieve good contour tracking is to have the y- axis sacrifice some of the performance available to it in order to better match the performance of the slower x-axis.

5. CONCLUSIONS

In this paper, a novel cross-coupled non-lifted norm optimal iterative learning control (cross-coupled NNOILC) approach has been proposed. By applying the proposed approach to a robotic multi-axis system, the contour error can be noticeably improved. This was demonstrated on an experimental system. Comparing the presented approach to existing cross-coupled NOILC approaches, the omission of a lifted framework reduces the computational complexity associated with the algorithm's implementation. The properties of the proposed cross-coupled NNOILC approach are also analyzed, including convergence, robustness, and computational complexity.

ACKNOWLEDGEMENT

This work was supported in part by the International Cooperation Program (Grant # 61120106009) of the National Science Foundation of China.

REFERENCES

Amann, N. Owens, D.H. and Rogers, E. (1996). Iterative learning control for discrete-time systems with exponential rate of convergence. *IEE Proceedings Control Theory Applications*, **143(2)**, 217–224.

Arimoto, S. Kawamura, S. and Miyazaki, F. (1984). Bettering operation of robots by learning. *Journal of Robotics Systems*, **1(2)**, 123-140.

Barton, K. and Alleyne, A. (2008). A cross-coupled iterative learning control design for precision motion control. *IEEE Trans. Control Syst. Technol.*, 16(6),1218-1231.

Barton, K. and Alleyne, A. (2011). A norm optimal approach to time-varying ILC with application to a multi-axis robotic testbed. *IEEE Trans. Control Syst. Technol.*, **19(1)**, 166–180.

Barton, K. Bristow, D. and Alleyne, A. (2010). A numerical method for determining monotonicity and convergence rate in iterative learning control. *Int. J. Control*, **83(2)**, 219-226.

Barton, K. Hoelzle, D. Alleyne, A. and Johnson, A. (2009). Cross Coupled Iterative Learning Control of Dissimilar Systems. *Proceedings of ASME Dynamic Systems and Control Conference*, 2009–2727.

Barton, K. Hoelzle, D. Alleyne, A. and Johnson, A. (2011). Cross-coupled iterative learning control of systems with dissimilar dynamics: design and implementation. *Int. J. Control*, **84(7)**, 1223-1233.

Barton, K. Wijdeven, J. Alleyne, A. Bosgra, O. and Steinbuch, M. (2008). Norm optimal cross-coupled iterative learning control. *Proceedings of the 47th IEEE Conference on Decision and Control*, 3020-3025.

Bristow, D. and Alleyne, A. (2006). A high precision motion control system with application to microscale robotic deposition. *IEEE Trans. Control Syst. Technol.*, **14(6)**, 1008–1020.

Bristow, D. Tharayil, M. and Alleyne, A. (2006). A survey of iterative learning control: A learning-based method for high-performance tracking control. *IEEE Trans. Control Syst. Mag.*, **26(3)**, 96-114.

Koren, Y. (1980). Cross-coupled biaxial computer control for manufacturing systems. *Journal of Dynamic Systems, Measurement, and Control*, **102(4)**, 265-272.

Lee, J.H. Lee, K.S. and Kim, W.C. (2000). Model-based iterative learning control with a quadratic criterion for time-varying linear systems. *Automatica*, **36(5)**, 641–657.

Moore, K.L. (1993). *Iterative learning control for deterministic systems*. Springer, London.

Phan, M. and Longman, R. (1988). A mathematical theory of learning control for linear discrete multivariable systems. *Proc. of the AIAA/AAS astrodynamics conference*, 740–746.

Phan, M. Longman, R. and Moore, K. (2000). Unified formulation of linear iterative learning control. *Advances in the Astronautical Sciences*, **105**, 93-11.

Rice, J.K. and Verhaegen, M. (2010). A structured matrix approach to efficient calculation of LQG repetitive learning controllers in the lifted setting. *Int. J. Control*, **83(6)**, 1265–1276.

Sun, H. and Alleyne, A. (in press). A computationally efficient norm optimal iterative learning control approach for LTV systems. *Automatica*.

Tang, L. and Landers, R. (in press). Multi-axis Contour Control-the State of the Art. *IEEE Transactions on Control Systems Technology*.